XMM-Newton CCF Release Note

XMM-CCF-REL-121

EPIC Spectral Response Distribution

R. D. Saxton, D. Lumb

12 July 2002

1 CCF components

Name of CCF	VALDATE	Blocks changed	CAL VERSION	XSCS flag
EMOS1_QUANTUMEF_0012.CCF	2000-01-01	QE_TOTAL, QE_CCD1		NO
EMOS2_QUANTUMEF_0012.CCF	2000-01-01	QE_TOTAL, QE_CCD1		NO

2 Changes

The MOS quantum efficiencies (QE) have been modified to give a better fit to ground calibration data. The major change from the previous files is that the central CCD in the MOS-2 camera now has greater quantum efficiency than the central CCD of MOS-1 at high energies. This was previously modelled as an empirical bump in the MOS-2 QE curve in EMOS2_QUANTUMEF_0010.CCF but is now included as part of a semi-physical model.

3 Scientific Impact of this Update

The difference in the QE and hence the ARF of an on-axis source in the MOS cameras is shown in Figures 1–4. The effect of this change is to modify the QE of MOS-1 by upto 5% between 0.1 and 10 keV (Figure 1). This change is relative to the *q20* canned response matrices, e.g. *m1_thin1v9q20t5r6_all_15.rsp* and to ARFs generated using the file EMOS1_QUANTUMEF_0010.CCF (Figure 2).

The new MOS-2 QE has a large excess above 4 keV relative to the *q20* canned matrices, e.g. *m2_thin1v9q20t5r6_all_15.rsp* (Figure 3.) and this will be noticeable as a reduction in high energy flux obtained from spectral fits of 5–10%. The change from EMOS2_QUANTUMEF_0010.CCF to EMOS2_QUANTUMEF_0012.CCF is upto 5% between 0.1 and 10 keV (Figure 4).

The ratio of the QE curves for the central CCD of the MOS detectors is shown in Figure 5.

4 Estimated Scientific Quality

These revised data were obtained from a re-analysis of the quantum efficiencies measured at the Orsay Synchrotron calibration campaigns. Individual QE vs. Energy data points were subject to statistical errors of several %.

For each CCD (ignoring for the time being spatial variations), the high energy absorption were well-characterised by an effective detection depth. This is not the same as a "true" depletion depth, as we are selecting (via. an energy-dependent mechanism) patterns 0-12, however the fit of the whole QE curves for E$\geq$4–5 keV is very well matched to a single detection depth. In addition the various fits cluster around two different depths, and these are very well correlated to the known distribution of CCDs from two different batches of silicon. The likely discrepancy in QE at highest (10keV) energies is of order 2–3%.

Once this effective depth is selected the rest of the QE is fit to a simple absorption model for the electrode side. In fact the inferred stopping depth does not translate well for the QE in the range 1.2-1.8keV, which is not unexpected because the event selection is not characterised well for the same stopping depth at these lower energies. The absorption in electrodes is characterised via. nominal widths of different electrode structures, and thicknesses of nitride, gate oxide, polysilicon and thermally grown oxide layers. Their thicknesses are leveraged by the depth of oxygen, silicon and nitrogen absorption edges, and also the general shape of the measured curve. The best fit curve with sensible absorbing structure depths is then merged to the high energy curve to produce the desired QE data file. For the soft X-ray efficiency, the biggest discrepancies are just below and above the Si edge, around the O edge, and at energies less than 200eV. Discrepancies of 10% between the experimentally measured points and the predicted curve occur at these limited regions.

5 Expected Updates

New curves have been generated for the central CCD in the MOS cameras. This work should be extended to the outer CCDs in a future release.

6 Test procedures

Find the flux in various energy bands of a bright, non-piled-up, on-axis source using canned matrices and the ARF produced by arfgen using these QE files. The results should be consistent with Figures 1–4.

Table 1: **Mos-1: fluxes derived from fits to an AGN spectrum**

Response	Inband flux[a]			
	0.5–2	2–3	2–5	5–10
Canned[b]	3.29	1.07	2.62	3.05
arfgen[c]	3.30	1.09	2.67	3.03
Change	0%	2%	2%	-1%

[a] The flux, in ergs s^{-1} cm^{-2}, returned by spectral fitting in the bands, 0.5–2 keV, 2–3 keV, 2–5 keV and 5–10 keV.
[b] The canned response file used was m1_medv9q20t5r6_all_15.rsp.
[c] The spectral fit used the canned response, m1_r6_all_15.rmf, in conjunction with an ARF produced by arfgen V1.48.10 (SAS V5.3.3) using the CCF, EMOS1_QUANTUMEF_0012.CCF, with the encircled energy correction turned off.

Table 2: **Mos-2: fluxes derived from fits to an AGN spectrum**

Response	Inband flux[a]			
	0.5–2	2–3	2–5	5–10
Canned[b]	3.33	1.05	2.53	2.83
arfgen[c]	3.33	1.07	2.54	2.62
Change	0%	2%	0%	-8%

[a] The flux, in ergs s^{-1} cm^{-2}, returned by spectral fitting in the bands, 0.5–2 keV, 2–3 keV, 2–5 keV and 5–10 keV.
[b] The canned response file used was m2_medv9q20t5r6_all_15.rsp.
[c] The spectral fit used the canned response, m2_r6_all_15.rmf, in conjunction with an ARF produced by arfgen V1.48.10 (SAS V5.3.3) using the CCF, EMOS2_QUANTUMEF_0012.CCF, with the encircled energy correction turned off.

7 Test results

The flux found from spectral fits to an AGN spectrum for the MOS cameras using the canned matrices and ARFs generated by arfgen using the new CCFs are shown in Tables 1 and 2.

The percentage changes for MOS-1 and MOS-2 agree qualitatively with those expected from the QE differences seen in Figures 1 and 3.

NB: The differences seen in these energy bands do depend on the source spectrum but the values quoted here are indicative of the magnitude of the change which will be seen in a typical source.

References

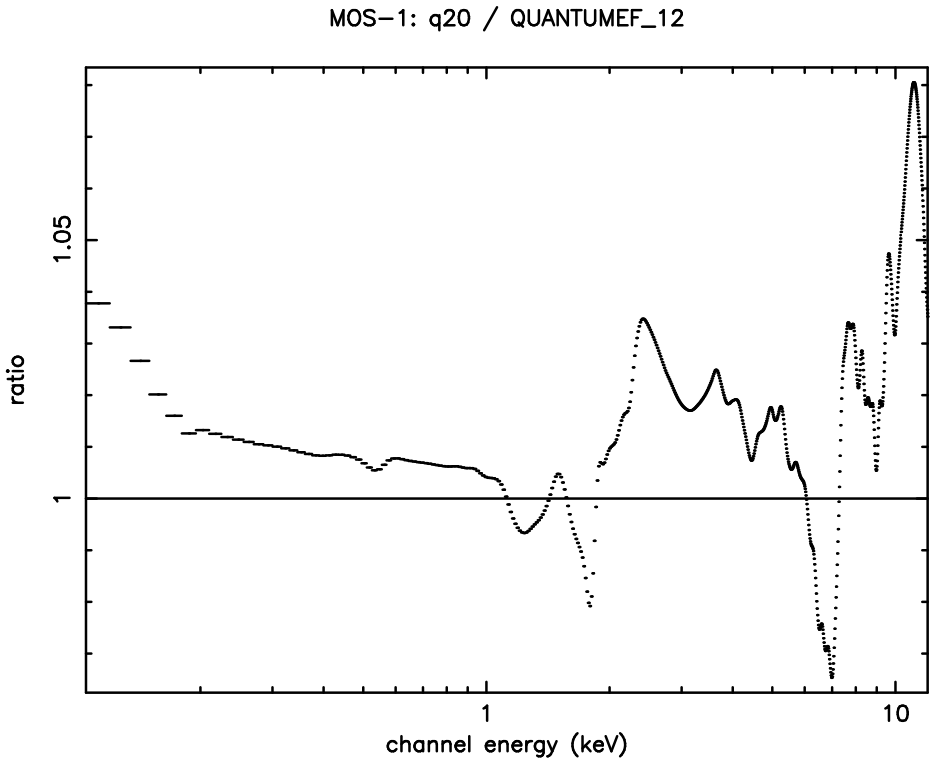

Figure 1: Comparison of the canned matrix, m1_medv9q20t5r6_all_15.rsp, MOS-1 response to a slope=1.5 power-law spectrum, with that of the SAS using the quantum efficiency file, EMOS1_QUANTUMEF_0012.CCF

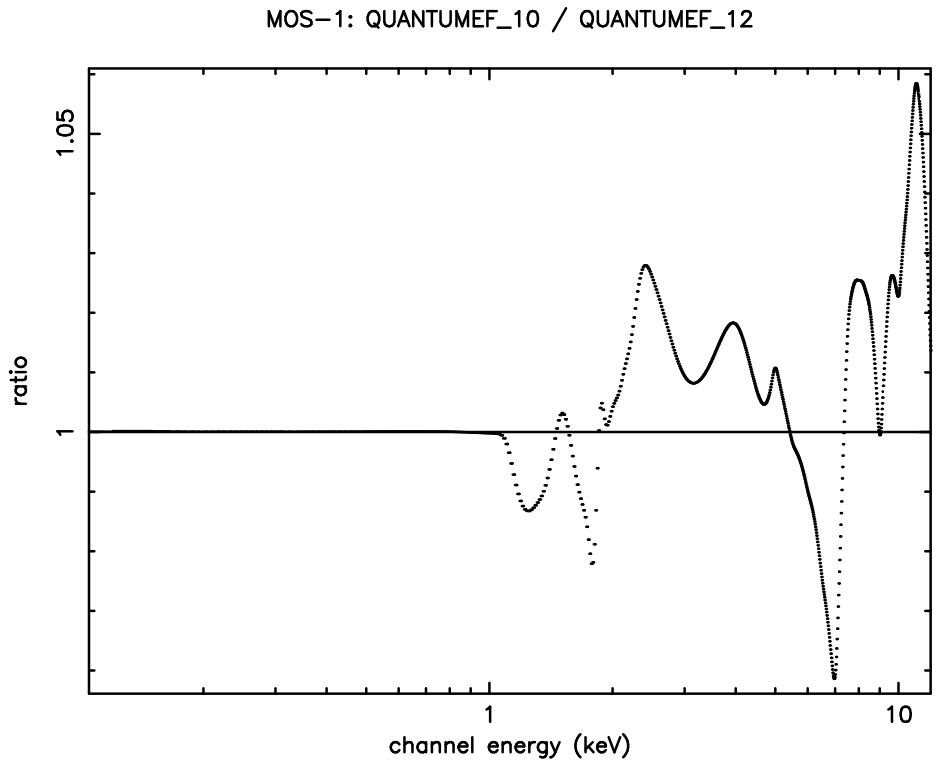

Figure 2: Comparison of the MOS-1 response to a slope=1.5 power-law spectrum, using the quantum efficiency files, EMOS1_QUANTUMEF_0010.CCF and EMOS1_QUANTUMEF_0012.CCF

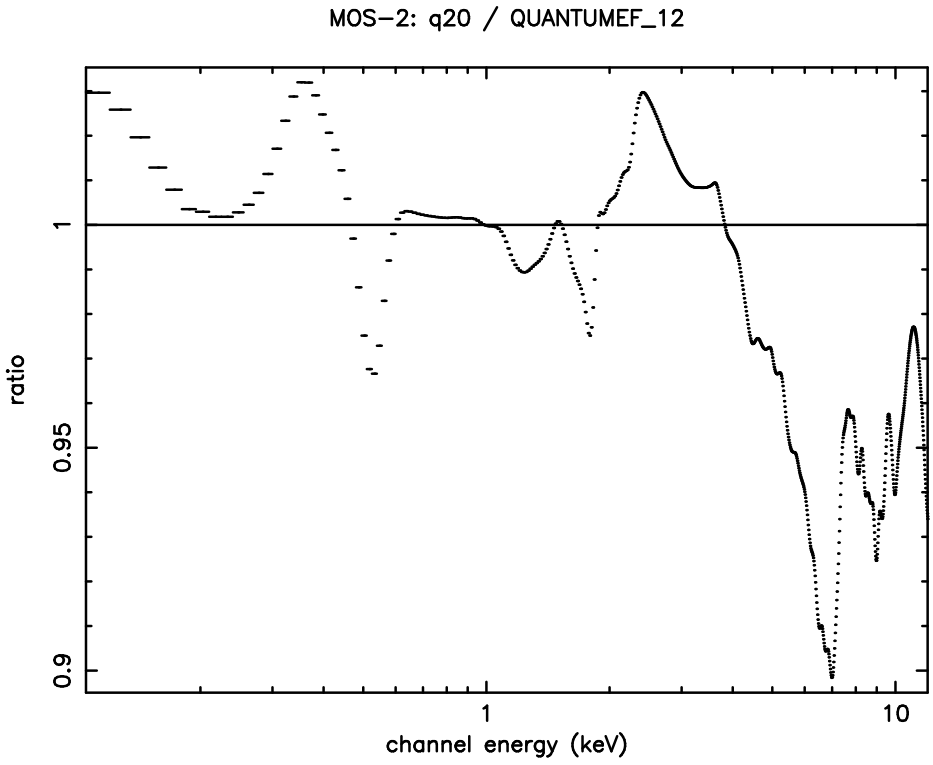

Figure 3: Comparison of the canned matrix, m2_medv9q20t5r6_all_15.rsp, MOS-2 response to a slope=1.5 power-law spectrum, with that of the SAS using the quantum efficiency file, EMOS2_QUANTUMEF_0012.CCF

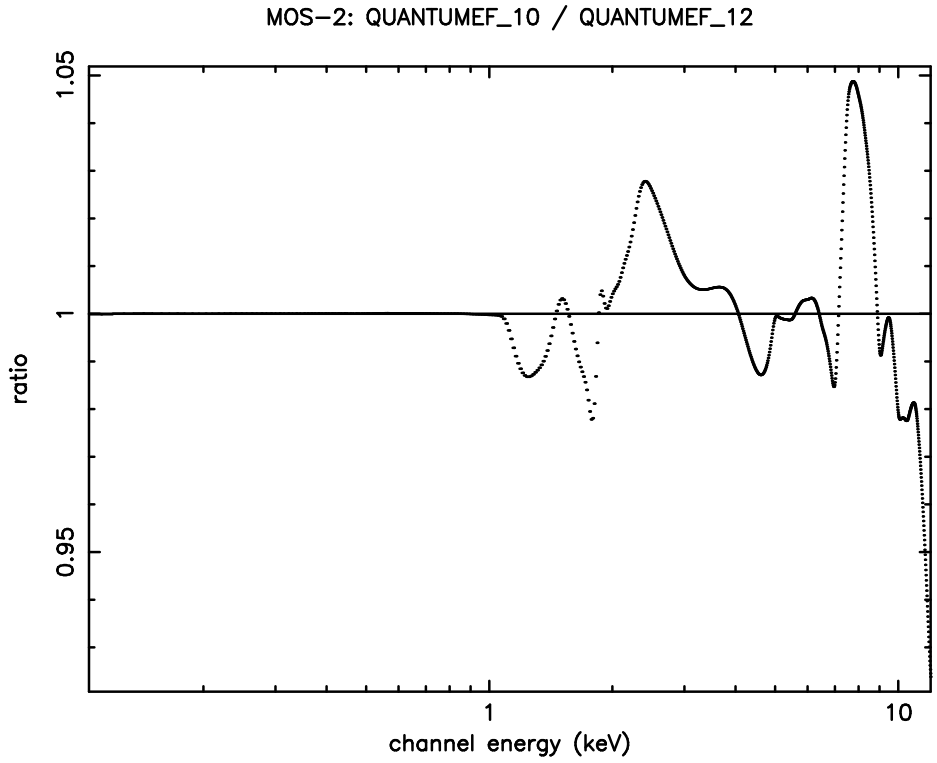

Figure 4: Comparison of the MOS-2 response to a slope=1.5 power-law spectrum, using the quantum efficiency files, EMOS2_QUANTUMEF_0010.CCF and EMOS2_QUANTUMEF_0012.CCF

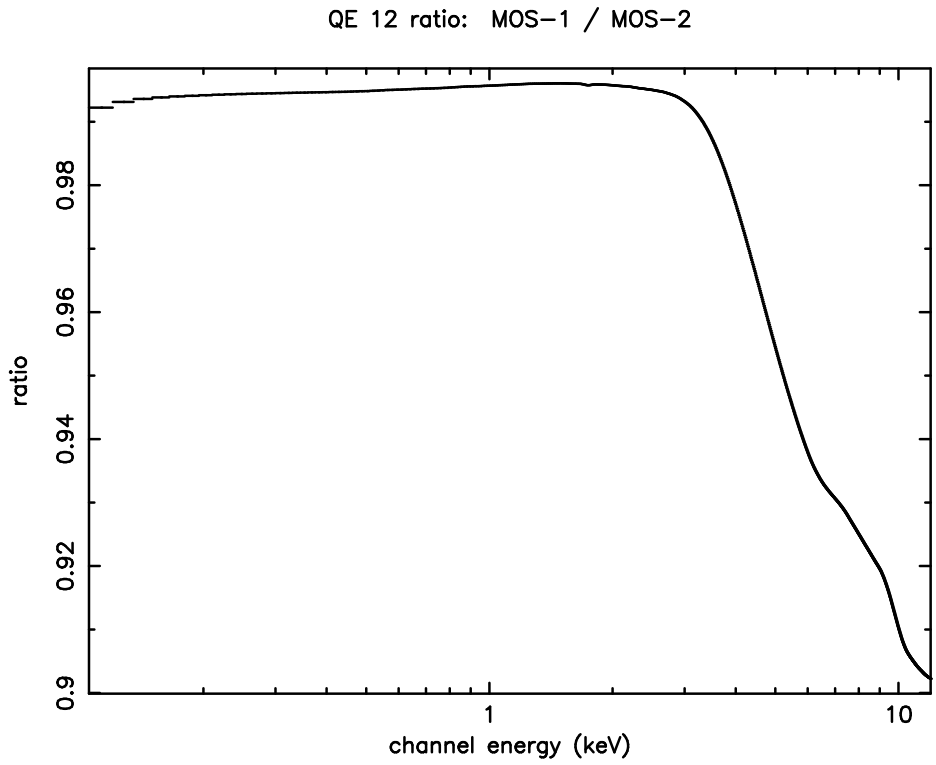

Figure 5: The relative quantum efficiencies of the central CCD of the MOS cameras given by the CCFs EMOS1_QUANTUMEF_0012.CCF and EMOS2_QUANTUMEF_0012.CCF